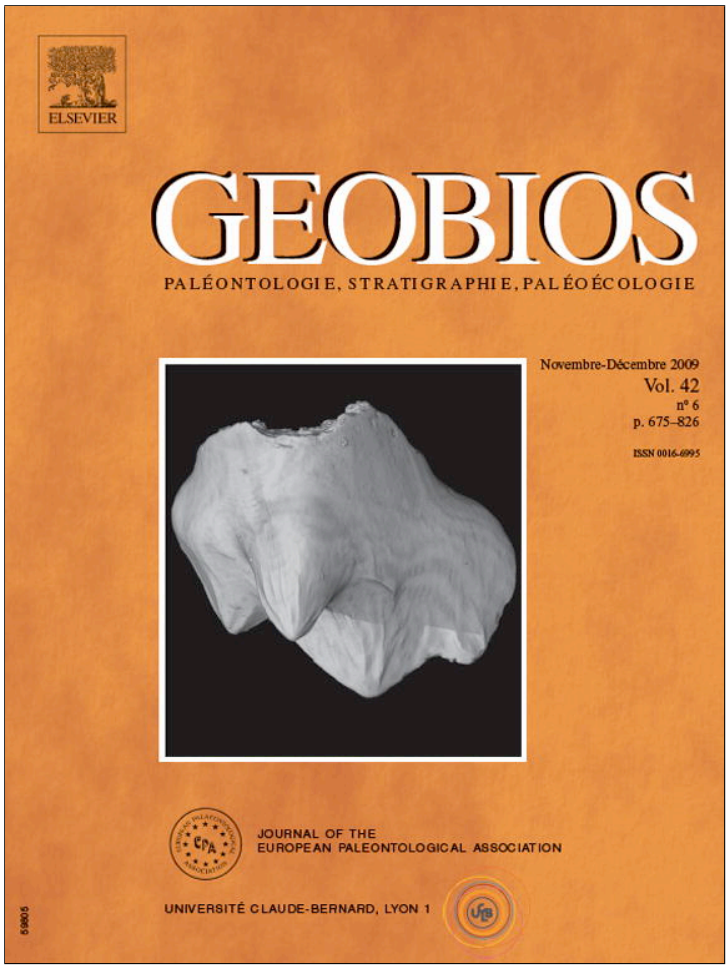

Disponible en ligne sur ScienceDirect www.sciencedirect.com

Elsevier Masson France EM|consulte www.em-consulte.com

ELSEVIER

GEOBIOS

Geobios 42 (2009) 699–714

Article original

Calcareous nannofossil productivity and carbonate production across the Middle-Late Jurassic transition in the French Subalpine Basin☆

Productivité des nannofossiles calcaires et production carbonatée à la transition Jurassique moyen-supérieur dans le bassin Subalpin français

Fabienne Giraud

UMR-CNRS 5125, « Paléoenvironnements et Paléobiosphère », campus de la Doua, université Lyon-1, rue Raphaël-Dubois, 69622 Villeurbanne cedex, France

Received 9 December 2008; accepted 26 May 2009
Available online 30 September 2009

Abstract

The distribution pattern of calcareous nannofossils was analysed across the Middle-Late Jurassic transition in the French Subalpine Basin (south-eastern France). This basin is characterized in the hemipelagic-pelagic domain by a continuous sedimentary succession, allowing a good biostratigraphic resolution for this time interval. The nannofossil assemblages are consistently dominated by *Watznaueria britannica*. However, major changes in trophic and paleoenvironmental conditions are recorded across the Middle-Late Jurassic transition. An increase in marine primary productivity and cooling of surface waters is recorded across the Callovian-Oxfordian boundary, as already shown in the higher latitude setting of the eastern Paris Basin. Increased precipitation and runoff under contrasting seasonal climatic conditions (monsoon-type) has led to eutrophication of marine surface waters in the French Subalpine Basin at this period. Then, decreased runoff and associated nutrients certainly linked to drier climatic conditions lead to a decrease in calcareous nannofossil productivity during the middle part of the Early Oxfordian (*mariae-cordatum* ammonite Zone transition). At the Early-Middle Oxfordian transition, more favourable conditions for the nannofossil community (warmer and mesotrophic surface waters) prevailed. The pelagic (nannofossil) carbonate contribution is limited, and the carbonate fraction is predominantly of nektonic/benthic origin at the Callovian-Oxfordian transition and of allochthonous origin from carbonate platforms at the Early Oxfordian-Middle Oxfordian transition.

Keywords: Calcareous nannofossil productivity; Middle-Late Jurassic transition; French Subalpine Basin; Paleoenvironmental changes; Carbonate production

Résumé

La distribution des nannofossiles calcaires dans le bassin subalpin français (Sud-Est de la France) a été analysée à la transition Jurassique moyen-supérieur. Ce bassin est caractérisé dans le domaine hémipélagique et pélagique par une sédimentation pratiquement continue pour cet intervalle de temps, permettant une bonne résolution biostratigraphique. Les assemblages de nannofossiles calcaires sont dominés par *Watznaueria britannica*. Cependant, des changements majeurs dans la fertilité des eaux de surface et dans les conditions paléoenvironnementales sont enregistrés à la transition Jurassique moyen-supérieur. Une augmentation de la productivité primaire marine associée à un refroidissement des eaux de surface est enregistrée à la transition Callovien-Oxfordien, comme cela avait déjà été montré dans le bassin Parisien. Durant cette période, des conditions climatiques périodiques de type mousson prévalaient dans cette zone, permettant une altération continentale importante et une augmentation des apports de nutriments dans les eaux de surface du bassin. Puis, au cours de l'Oxfordien inférieur, une réduction des apports silicoclastiques et des nutriments associés, entraîne une diminution importante de la productivité des nannofossiles calcaires. Cette réduction des apports continentaux est certainement liée à des conditions climatiques devenant plus arides. Un réchauffement des eaux de surface et des conditions mésotrophes caractérisent ensuite la transition Oxfordien moyen-supérieur dans le bassin Subalpin. La contribution des nannofossiles calcaires à la fraction carbonatée et l'origine pélagique du carbonate en général, reste toujours limitée. À la transition Callovien-Oxfordien, la fraction carbonatée du sédiment est principalement d'origine autochtone, et provient pour l'essentiel de coquilles d'organismes nectoniques et/ou

☆ Corresponding editor: Gilles Escarguel.

E-mail address: Fabienne.Giraud@univ-lyon1.fr.

0016-6995/$ – see front matter
doi:10.1016/j.geobios.2009.05.002

benthiques. À la transition Oxfordien moyen-supérieur, le carbonate a une origine essentiellement allochtone, en provenance des aires de plate-forme peu profondes.

Mots clés : Productivité des nannofossiles calcaires ; Transition Jurassique moyen-supérieur ; Bassin Subalpin français ; Changements paléoenvironnementaux ; Production carbonatée

1. Introduction

The Late Callovian-Early Oxfordian interval is characterized by a cool climatic phase (Dromart et al., 2003). During this period, the general absence of carbonate sediments and the lack of reef formations reflect a crisis in the carbonate production (Cecca et al., 2005). The presence of numerous stratigraphic hiatus across the Callovian-Oxfordian boundary could be the result of an abrupt sea-level fall, with a minimum in the Late Callovian (*lamberti* ammonite Zone; Dromart et al., 2003).

Coral-reef distribution, ammonite biogeographical patterns, paleofloral assemblages and geochemical data (synthesis in Cecca et al., 2005) document the onset of progressive warming associated with a long-term sea-level rise during the Middle Oxfordian. Across the Early/Middle Oxfordian boundary, major plate tectonic reorganisation and consequently major paleoceanographic and climatic changes occur. Low $^{87}Sr/^{86}Sr$ values are recorded, reflecting a major pulse of hydrodynamism related to the onset of rifting in the North and South Atlantic regions (Jones et al., 1994). Neodynium isotopic signatures of phosphatic sediments also indicate that at that time, Tethyan and Central Atlantic oceanic waters were similar to Pacific waters in composition (Stille et al., 1996). The opening of an oceanic gateway between the equatorial Tethys-Atlantic and Pacific oceans provided a substantial flow of warmer ocean water and initiated an ocean current system, which effectively exported heat from low to high latitudes (Hotinski and Toggweiler, 2003), influencing Northern Tethyan and Boreal basins located at middle latitudes (Louis-Schmid et al., 2007b).

Despite their great potential for paleoceanographic reconstructions, only one previous work deals with calcareous nannofossil assemblages encountered during this period of major climatic and paleoenvironmental changes (Tremolada et al., 2006). Poor biostratigraphic resolution of the very condensed deposits observed in the Western Tethys during this time interval can explain the limited number of quantitative studies. Nevertheless, Tremolada et al. (2006) have shown that in the eastern Paris Basin, calcareous nannofossils record an increase of primary productivity at the Callovian-Oxfordian transition in relation with the cooling phase.

The aim of this work is to analyse the distribution pattern of the calcareous nannofossils in the French Subalpine Basin (south-eastern France) during the Middle-Late Jurassic transition in order to see:

- whether the primary productivity also increases in this basin;
- the response of nannofossil (productivity and pelagic carbonate production) to climatic changes (transition from cooling phase to progressive warming).

The French Subalpine Basin is located at a lower latitude than the eastern Paris Basin and is characterized by an almost continuous temporal sedimentary succession in the hemipelagic-pelagic domain, allowing a good biostratigraphic resolution for the Middle-Late Jurassic interval.

2. Regional setting

The French Subalpine Basin belongs to the North Tethyan margin and was located between 30° and 35°N across the Middle-Late Jurassic transition (Fig. 1). This basin underwent

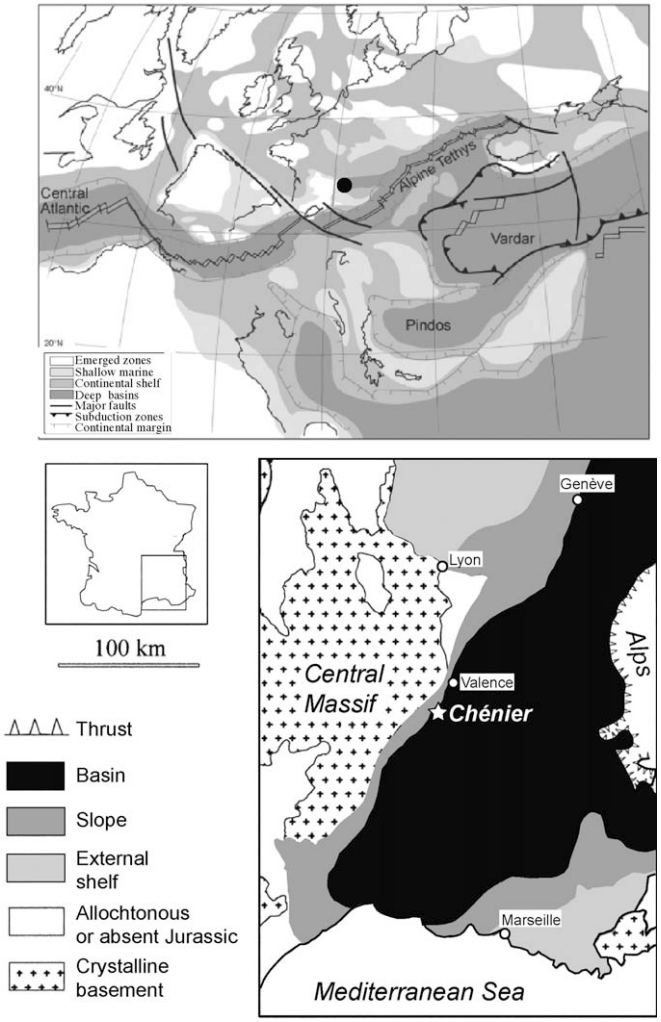

Fig. 1. Callovian-Oxfordian paleogeographic map (Stampfli et al., 2001), showing the location of south-eastern France and paleogeographic setting of the Chénier Ravine section. The paleogeography of south-eastern France is from Bouhamdi et al. (2000) and corresponds to the Middle Oxfordian.

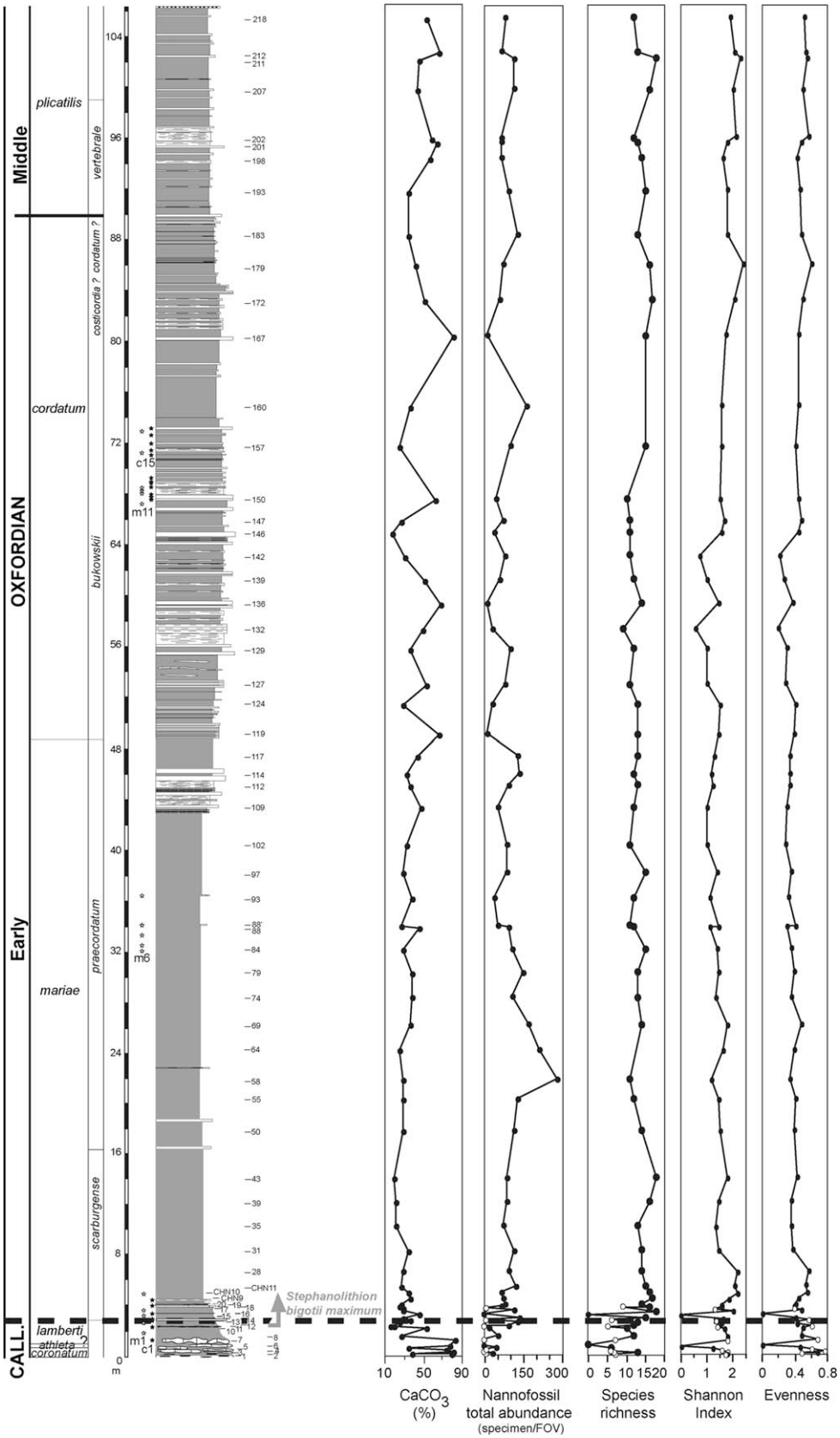

Fig. 2. Stratigraphic changes in calcium carbonate content, calcareous nannofossil total abundance (specimens per field of view), species richness, and Shannon diversity and evenness for the Chénier Ravine section. Ammonite biostratigraphy after Elmi (1967); calcareous nannofossil events after this work. Positions of samples selected for carbonate contents and calcareous nannofossil studies are shown. White dots correspond to poorly preserved samples with strongly etched and/or overgrown nannofossil assemblages. Small stars located at the left of the lithostratigraphic column indicate the position of thin sections (black stars: limestone samples; white stars: marl samples).

extensional or strike-slip faulting, inherited from Tethyan rifting (Lemoine and de Graciansky, 1988; de Graciansky et al., 1999). Differentially subsiding faults and tilted blocks induced heterogeneous subsidence and significant thickness variations across the basin and its margin (Dardeau et al., 1994; Nyman et al., 1996). During the Middle Jurassic, the accelerated subsidence provided much accommodation space in the French Subalpine Basin (Dardeau et al., 1994) and allowed the deposition of the 'Terres Noires' Formation (Artru, 1972). These silty black marls range in thickness from a few tens to over a thousand metres (Debrand-Passard et al., 1984). Two sedimentary intervals are recognized in the 'Terres Noires' Formation (Artru, 1972), resulting from combined effects of extensional tectonics and eustacy (Dardeau et al., 1988).

The biostratigraphy of the 105 m-thick studied Chénier Ravine section (Fig. 2) was established by Elmi (1967) and is based on ammonite biozonation. The analysed succession is dated from the Middle Callovian (*coronatum* ammonite Zone) to the Middle Oxfordian (*plicatilis* ammonite Zone). The first 2 m of the section are characterized by slumped calcareous beds of Middle-Late Callovian age possibly generated by synsedimentary slides (Elmi, 1990). Above these slumps starts the first interval of the Late Callovian 'Terres Noires' Formation. It corresponds to 3 m of grey marls with red or grey nodular calcareous beds or argillaceous limestones. Thin ferruginous levels are present in marls and limestones. Above these first 3 m, the 'Terres Noires' Formation becomes marly and consists of nearly 40 m of early Oxfordian grey argillaceous marls, in which scarce thin calcareous beds are intercalated. Upwards of the section, there is a progressive transition from the 'Terres Noires' Formation to marl-limestone alternations typical of the Middle Oxfordian.

The paleoenvironment of the Chénier area corresponds to the upper part of the bathyal zone near the slope-basin transition (Charbonnier et al., 2007).

3. Methods

Carbonate content was measured in 69 samples corresponding to different lithologies in the Chénier Ravine section (Fig. 2). Calcium carbonate content was determined using the carbonate bomb technique, which measures CO_2 emission during a hydrochloric acid attack.

Calcareous nannofossils were analysed in the same 69 samples as for $CaCO_3$ estimates (Fig. 2). Simple smear slides were prepared for biostratigraphic analysis and nannofossil quantification. Samples were prepared as homogeneously as possible so that particle densities in different slides were comparable. However, this preparation technique does not guarantee a perfectly homogeneous distribution and constant quantity of material on the smear slide. Thus, the density in each smear slide was calculated as the mean density of material in 12 fields of view randomly chosen at 500X magnification. In each of these fields of view, the percentage of material on the smear slide was estimated using the plates of Baccelle and Bosellini (1965). Successive tests have shown that the error in mean density estimates is lower than 5% (Pittet and Mattioli, 2002).

Different longitudinal transverses were observed under a light-polarising microscope, at 1560X magnification, in order to find biostratigraphic markers. For the quantification of nannofossils, 300 specimens were counted in a variable number of fields of view on the smear slide in the richest samples. In the poorest samples, specimens were counted following one or two longitudinal transverses. The number of views necessary to count them is used to calculate the total abundance of nannofossils in each sample, which corresponds to the number of specimens divided by the number of views necessary to count them. This abundance per view is then standardised to the density of material on the smear slide (Pittet and Mattioli, 2002). Relative abundance of each species was also calculated in each sample. The combination of semi-quantitative and relative abundances allows an accurate interpretation of nannofossil assemblage changes (Williams and Bralower, 1995). The taxonomy applied here follows the guidelines of Perch-Nielsen (1985) and Bown and Young (1997). Fifteen species and two morphotypes are considered for the semi-quantitative analysis. Together, they represent 72 to 97.7% of the total nannofossil assemblage, which is composed of 28 species. The nannofossil assemblage composition is also described by means of the species richness and Shannon Diversity Index and evenness (Shannon and Weaver, 1949). The nannofossil preservation was evaluated by using the simplified classes established by Roth (1983).

4. Results

The entire nannofossil dataset is given in Table S1 of Appendix A. All nannofossil taxa encountered in this study are reported in Appendix B; taxonomic remarks were added when needed. Some selected species are illustrated in Fig. 3.

4.1. Nannofossil biostratigraphy

The studied interval spans nannofossil Zones NJ13 through NJ15a, adopting the biozonation of Bown and Cooper (1998). Only one zonal marker, *Stephanolithion bigotii maximum*, is recognized (Fig. 2). The first occurrence of this marker is recognized within the *lamberti* ammonite Zone (top of the zone) both in Tethyan and Boreal domains (Bown et al., 1988). The boundary between *athleta* and *lamberti* ammonite Zones is not well constrained in the Chénier Ravine section, and our observations suggest that the base of *lamberti* ammonite Zone occurs lower than sample 12 (Fig. 2). The last occurrence of *Stephanolithion bigotii maximum* is reported at the top of the Early Oxfordian (*cordatum* ammonite Zone) in NW Europe and in Switzerland (Bown and Cooper, 1998), while it falls within the underlying *mariae* Zone in SE France, suggesting diachronism (de Kaenel et al., 1996). This marker is present at the top of the Chénier Ravine section, assigned to the Middle Oxfordian (lower part of the *plicatilis* ammonite Zone), suggesting that the stratigraphic extension of this taxon could

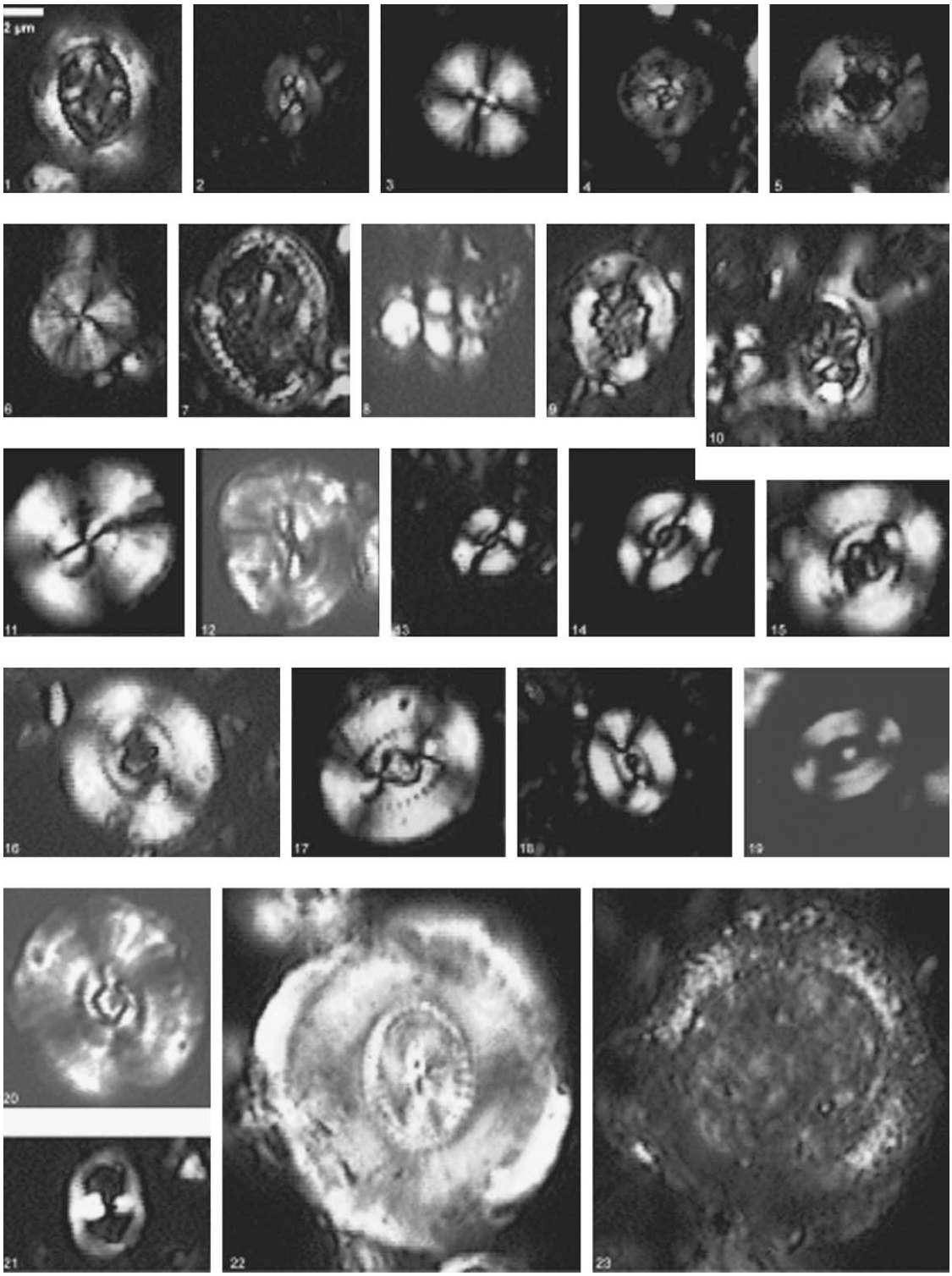

Fig. 3. Light microscope pictures of selected nannofossil species from the Chénier Ravine section. **1**. *Axopodorhabdus cylindratus* (Noël, 1965) Wind and Wise in Wise and Wind, 1976. **2**. *Biscutum dubium* (Noël, 1965) Grün in Grün et al., 1974. **3**. *Cyclagelosphaera margerelii* (Noël, 1965). **4**. *Discorhabdus* sp. **5**. *D. patulus* (Deflandre in Deflandre and Fert, 1954) Noël, 1965. **6**. *D. striatus* Moshkovitz and Ehrlich, 1976. **7**. *Ethmorhabdus gallicus* Noël, 1965 (Fig. 3). **8**. *L. hauffii* Grün and Zweili in Grün et al., 1974. **9**. *Polypodorhabdus escaigii* Noël, 1965. **10**. *Stephanolithion bigotii* Deflandre, 1939 ssp. *maximum* Medd, 1979. **11**. *Watznaueria barnesiae* (Black, 1959) Perch-Nielsen, 1968. **12**. *Watznaueria* aff. *barnesiae*. **13–19**. *W. britannica* (Stradner, 1963) Reinhardt, 1964; 13, Morphotype A; 14, Morphotype B; 15, Morphotype C; 16, Morphotype D; 17, Morphotype E; 18, Morphotype F; 19, Morphotype G. **20**. *W. manivitiae/britannica*. **21**. *Z. erectus* (Deflandre in Deflandre and Fert, 1954) Reinhardt, 1965. **22**. *W. manivitiae* Bukry, 1973. **23**. *Schizosphaerella punctulata* Deflandre and Dangeard, 1938.

be more important than reported by previous works and that its last occurrence is not reliable for biostratigraphic correlations.

4.2. Nannofossil assemblages

In general, preservation of nannofossils is moderate with moderately etched and/or overgrown nannofossil assemblages (see Table S1). Samples 6 and 16 are barren of nannofossils. At the base of the Chénier Ravine section, some samples are poorly preserved with strongly etched and/or overgrown assemblages. Few samples are characterized by slightly etched and/or overgrown nannofossils.

The nannofossil assemblages are dominated by *Watznaueria* spp. (Fig. 4), which represent more than 80% of the assemblage; within the *Watznaueria* group, *W. britannica* dominates (Fig. 4). *Watznaueria britannica* presents seven morphotypes described in Giraud et al. (2006, 2009) (Fig. 4). The small morphotypes (A + B) are always dominant throughout the succession, and within the large morphotypes, E and D are well represented. The other *Watznaueria* are mainly represented by *W. barnesiae/fossacincta*; these two species are grouped because they are believed to represent end-members of a morphological continuum (Lees et al., 2004, 2006; Bornemann and Mutterlose, 2006). Two other large *Watznaueria* morphotypes, frequent to common in the assemblages, are recognized in this study and described in Giraud et al. (2009). The first one is *W. manivitiae/britannica*, and the second one is *W.* aff. *barnesiae*. *W. manivitiae* is rare to frequent in the assemblages. Other rare species of *Watznaueria* are grouped (''other *Watznaueria*'' in Fig. 4). The other coccoliths significantly contributing to the nannofossil assemblage are in decreasing order of abundance: *Cyclagelosphaera margerelii*, *Biscutum dubium*, *Discorhabdus* spp. (*D.* sp., *D. striatus* and *D. patulus*), *Lotharingius hauffii,* the Axopodorhabdaceae, defined by Tremolada et al. (2006) as the A-group (*Axopodorhabdus* spp., *Etmorhabdus gallicus* and *Polypodorhabdus escaigii*), and *Zeugrhabdotus erectus*. The nannofossil *incertae sedis Schizosphaerella punctulata* is also present.

Distinctive distribution patterns of calcareous nannofossils are recognized throughout the studied succession associated with changes in calcium carbonate content.

From the Middle Callovian until the Callovian-Oxfordian boundary, the calcium carbonate content sharply decreases, and the mean nannofossil total abundance is very low in limestones (across three specimens per field of view) and around 56 specimens per field of view in marls (Fig. 2). Species richness is also lower in limestone beds (mean value of 6) than in marls (mean value of 10; Fig. 2). Shannon diversity is low (mean values of 1.5), and the average evenness is 0.5 (Fig. 2). The relative abundances of *Watznaueria barnesiae/fossacincta* and of *Schizosphaerella punctulata* decrease during this interval (Fig. 4).

Across the Callovian-Oxfordian boundary, the mean calcium carbonate is low (30%), and the mean nannofossil total abundance increases (112 specimens per field of view; Fig. 2). Species richness increases (mean value of 14), whereas the Shannon diversity is always low (mean value of 1.5) and the evenness decreases (mean value of 0.4; Fig. 2). The relative proportion of *W. britannica* increases, and the contribution of large-sized *W. britannica* (Morphotype D and E) is important (Fig. 4). *Cyclagelosphaera margerelii* presents its highest percentage just below the Callovian-Oxfordian boundary. In the rest of the assemblage, *B. dubium*, *Z. erectus*, the A-group and *Discorhabdus* spp. present their highest relative abundance just above the boundary.

The middle part of the Early Oxfordian (*mariae-cordatum* ammonite Zones transition) is characterized by a slight increase in the calcium carbonate content (mean value of 42%), a decrease in both mean nannofossil total abundance (71 specimens per view), mean species richness (12 species) and mean Shannon diversity indices (1.1 and 0.3 for Shannon index and evenness, respectively; Fig. 2). Almost all taxa decrease during this interval (Fig. 4). The assemblages are dominated by small-sized *W. britannica*, and *W. manivitiae/britannica* display a maximum in their relative abundances.

From the upper part of the Early Oxfordian until the early Middle Oxfordian, the calcium carbonate content (mean value of 47%), the mean nannofossil total abundance (84 specimens per view), the species richness (mean value of 14 species) and the diversity indices (1.8 and 0.5 for Shannon index and evenness, respectively) all increase (Fig. 2). The relative abundance of *Watznaueria britannica* decreases with a lower contribution of small-sized specimens (Morphotypes A and B) and a higher contribution of Morphotype E (Fig. 4). The relative abundance of *C. margerelii* and of the A-group decreases during this interval. The relative abundances of ''other *Watznaueria*'' and *W. manivitiae* slightly increase, whereas those of *Discorhabdus* spp. and *L. hauffii* strongly increase.

The correlation indices between distinctive variables are shown in Fig. 5. We have excluded from this analysis samples presenting strongly etched and/or overgrown assemblages. We have considered two groups of *W. britannica*, small *W. britannica* (Morphotypes A + B) and large *W. britannica* (other morphotypes), based on previous studies showing that ecological preferences of the small and large specimens were different (Olivier et al., 2004; Lees et al., 2005; Tremolada et al., 2006; Giraud et al., 2006). Within the *W. britannica* assemblage, the relative abundance of small morphotypes displays high negative correlation with Shannon diversity index and evenness, significant negative correlation with species richness and the relative abundances of large morphotypes and of *Discorhabdus* spp., and low negative correlation with *W. manivitiae*, *C. margerelii* and *W.* aff. *barnesiae*. The percentage of *W. barnesiae/fossacincta* shows positive correlation with *S. punctulata* and low negative correlation with *B. dubium*. The relative abundance of *W.* aff. *barnesiae* displays positive correlation with *C. margerelii* and *Z. erectus* and low negative correlation with *W. manivitiae/britannica*. The percentage of *Discorhabdus* spp. shows positive correlation with *B. dubium*, *L. hauffii* and *W. manivitiae*, and both positively correlate with Shannon diversity and evenness. The relative abundance of the A-group displays positive correlation with nannofossil total abundance (specimens/field of view) and species richness.

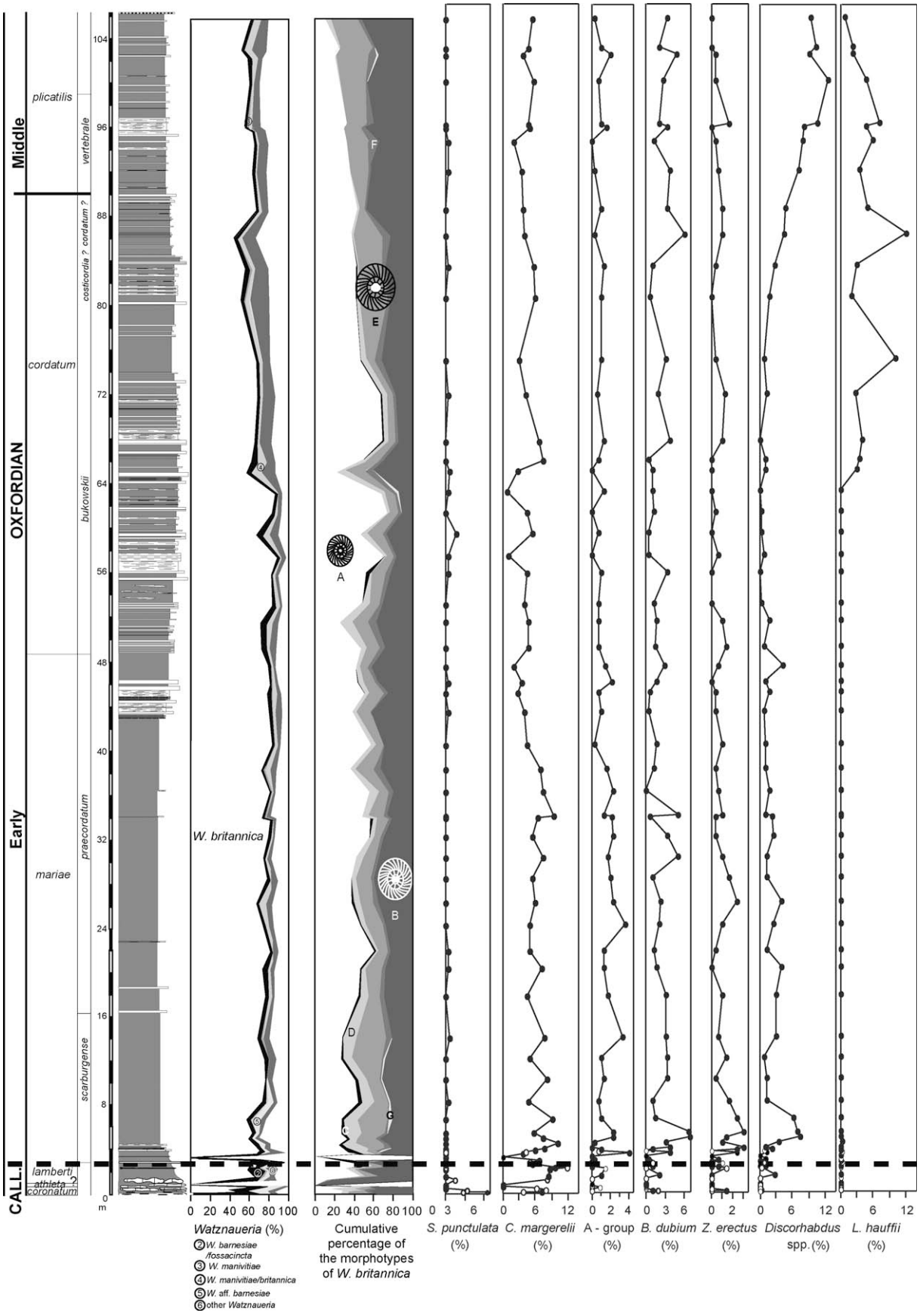

Fig. 4. Relative abundance curves of *Watznaueria* species with respect to the entire nannofossil assemblage, compared to the percentage of each morphotype of *W. britannica* within the *W. britannica* assemblage and to the percentage of selected nannofossil taxa for the Chénier Ravine section. White dots correspond to poorly preserved samples with strongly etched and/or overgrown nannofossil assemblages.

	small *W. britannica* (%)	large *W. britannica* (%)	*W. barnesiae/fossacincta* (%)	*W.* aff. *barnesiae* (%)	*W. manivitiae/britannica* (%)	*W. manivitiae* (%)	*C. margerelii* (%)	*L. hauffii* (%)	*B. dubium* (%)	*Discorhabdus* spp. (%)	A-group (%)	*Z. erectus* (%)	*S. punctulata* (%)	Nanno. Tot. Ab. (sp/FOV)	Species richness	Shannon Index	Evenness	$CaCO_3$ (%)
small *W. britannica* (%)	1.000																	
large *W. britannica* (%)	**-0.63**	1.000																
W. barnesiae/fossacincta (%)	-0.157	-0.171	1.000															
W. aff. *barnesiae* (%)	**-0.33**	**0.396**	0.107	1.000														
W. manivitiae/britannica (%)	-0.096	-0.085	-0.202	**-0.392**	1.000													
W. manivitiae (%)	**-0.367**	0.217	-0.03	-0.072	0.078	1.000												
C. margerelii (%)	**-0.358**	**0.343**	0.046	**0.466**	-0.164	-0.016	1.000											
L. hauffii (%)	-0.323	-0.168	-0.167	-0.244	0.192	0.191	-0.246	1.000										
B. dubium (%)	-0.294	0.236	**-0.332**	0.026	-0.21	-0.011	0.133	0.251	1.000									
Discorhabdus spp. (%)	**-0.499**	0.227	-0.269	-0.029	0.092	**0.375**	-0.017	**0.387**	**0.396**	1.000								
A-group (%)	0.067	0.102	-0.296	-0.118	-0.106	0.048	0.132	-0.195	0.303	0.076	1.000							
Z. erectus (%)	-0.274	0.313	0.014	**0.386**	-0.298	-0.039	0.261	-0.118	0.298	0.034	0.187	1.000						
S. punctulata (%)	-0.097	-0.039	**0.42**	-0.117	-0.004	-0.121	-0.032	-0.085	-0.219	-0.182	-0.178	-0.096	1.000					
Nanno. Tot. Ab. (sp/FOV)	0.188	0.009	-0.282	0.057	-0.051	-0.028	-0.068	-0.004	0.217	0.092	**0.357**	0.113	-0.215	1.000				
Species richness	**-0.519**	**0.532**	-0.301	0.259	-0.140	0.173	0.235	0.065	**0.401**	**0.344**	**0.394**	0.318	0.002	0.178	1.000			
Shannon Index	**-0.858**	0.328	0.047	0.253	0.087	**0.365**	0.316	**0.445**	**0.477**	**0.646**	0.153	0.323	-0.045	0.01	**0.626**	1.000		
Evenness	**-0.827**	0.195	0.22	0.198	0.134	**0.36**	0.275	**0.482**	**0.4**	**0.602**	0.038	0.261	-0.03	-0.056	**0.369**	**0.952**	1.000	
$CaCO_3$ (%)	-0.056	-0.247	-0.02	-0.324	0.178	0.111	-0.187	0.271	-0.145	0.264	-0.149	-0.263	0.063	**-0.412**	-0.119	0.067	0.104	1.000

Fig. 5. Correlation indices between the percentages of selected nannofossil taxa, nannofossil total abundance (specimens per field of view), species richness, Shannon diversity and evenness, and calcium carbonate contents. All correlations are based on a dataset of 60 samples; poorly preserved samples characterized by strongly etched and/or overgrown nannofossil assemblages, are excluded from this analysis. In bold, statistically significant values at the 0.01 significance level.

5. Discussion

5.1. Calcareous nannofossil preservation

The preservation state can control nannofossil abundance, species richness, and relative abundance of some species. Dissolution ranking of Cretaceous calcareous nannofossils has been proposed by several authors (Hill, 1975; Thierstein, 1980; Roth, 1981; Roth and Krumbach, 1986). Dissolution-resistant species are the large, thick placoliths with strongly imbricated elements (Hill, 1975), such as the *Watznaueria* group. *Watznaueria* is dominant throughout the time interval at the Chénier Ravine section. This dominance is also indicated by the Shannon index comprised between 0.61 and 2.4, corresponding to low diversity values (Frontier and Pichod-Viale, 1998). However, for the Callovian-Oxfordian interval, *Watznaueria* is dominant in poor to pristine nannofossil assemblages recovered from different latitudinal marine paleoenvironments (Table 1). This dominance in said time interval is certainly not the consequence of selective diagenesis. Among the *Watznaueria* species, *W. barnesiae* (thick coccolith, closed central area) is considered as one of the most resistant placoliths to dissolution (Hill, 1975; Thierstein, 1980, 1981; Roth, 1981; Roth and Bowdler, 1981; Roth and Krumbach, 1986). Thus, an increase in diagenetic alteration may imply an increase in the relative abundance of *W. barnesiae*. Because of its dominance in the Early Jurassic nannofossil assemblages and its high dissolution resistance, *Schizosphaerella* spp. is considered in terms of diagenetic resistance as an equivalent of *W. barnesiae* (Mattioli, 1997). Conversely, *Biscutum* spp. and *Z. erectus* are very fragile taxa (Hill, 1975; Thierstein, 1980; Roth, 1981, 1983): an increase of diagenetic overprint may imply a decrease in their relative abundance.

Four classes of preservation are recognized in the Chénier Ravine section (see Table S1):

- class 1, SE and/or SO (strongly etched and/or overgrown);
- class 2, ME-MO (moderately etched and overgrown);
- class 3, ME-sO or sE-MO (moderately etched-slightly overgrown or slightly etched-moderately overgrown);
- class 4, sE-sO (slightly etched and overgrown).

We have statistically tested the effect of the different classes of preservation observed on nannofossil total abundance, species richness, and relative abundance of *W. barnesiae* and the group of delicate taxa (*B. dubium* + *Z. erectus*). Highest mean in nannofossil total abundance is recorded in samples having a moderate degree of etching and/or overgrowth (Fig. 6(A)). Slightly higher species richness (Fig. 6(B)) and mean relative abundance of delicate taxa (Fig. 6(C)) are observed in samples presenting a small degree of etching and overgrowth. Highest mean relative abundances of *W. barnesiae*

Table 1
General characteristics of calcareous nannofossil assemblages recovered for the Callovian-Oxfordian time interval, based on qualitative and/or quantitative published data.

Province	Location	Lithostratigraphy or lithology	Paleoenvironment	Calcareous nannofossils	Age	Paleolatitude[a]	Reference
Central Russia	Oka Riva Region	Dark grey shales	Epicontinental seaway	Well-preserved, dominance of *Watznaueria*; more than 20 species	Oxfordian	50°N	Rahman and Roth (1992)
Western Scotland	Isle of Skye Staffin bay	Staffin shales formation	Outer shelf	Bad to well-preserved, dominance of *W. britannica*; 21 species	Callovian-Oxfordian	44°N	Hamilton (1978)
Netherlands	Achterhoek area, Lower Saxony basin	Dark grey calcareous claystone	Marine close to the coast	Well-preserved, dominance of *W. britannica*; 13 species	Middle Callovian	43°N	Herngreen et al. (2000)
England	Haddenham and Gamlingay boreholes	Ampthill Elsworth Rock Group Oxford Clay Formations	Shallow epeiric sea	Well-preserved, dominance of *W. britannica*; more than 70 species	Callovian-Oxfordian	38°N	Medd (1979)
Central and Southern England	King's Dyke Pit	Peterborough Member Oxford Clay Formation	Shallow epeiric sea	Moderate to well-preserved, dominance of *W. britannica*; 29 species	Middle Callovian	38°N	Walsworth-Bell (2001)
Southern Germany	Western swabian Alb	Marls and limestones	Deep-shelf	Bad to well-preserved, dominance of *W. britannica* or *Schizosphaerella* spp.; 31 species	Late Oxfordian	37°N	Pittet and Mattioli (2002) Olivier et al. (2004)
Eastern Paris Basin	HTM 102 well	Argiles de la Woëvre Formation	Lower median to distal offshore	Moderate to well-preserved, dominance of *W. barnesiae/fossacincta*; 24 species	Late Callovian-Middle Oxfordian	35°N	Tremolada et al. (2006)
Southeastern France	Ardèche margin	Terres Noires Formation	Slope-basin transition	Bad to well-preserved, dominance of *W. britannica*; 29 species	Middle Callovian-Middle Oxfordian	30°N	This study
Central Atlantic	DSDP 534 A	Organic carbon-rich shales	Deep basin: deposition near the CCD	Bad-preserved, dominance of *W. barnesiae*; 23 species	Middle Callovian-Oxfordian	15°N	Roth (1983)
Southern Israel Northern Sinai	Northeastern Negev Gebel Maghara	Zohar, Kidod and Beer Sheba Formations	Peritidal	Moderate to well-preserved, dominance of *W. britannica* or *C. margerelii*; 15 species	Callovian-Oxfordian	8°N	Moshkovitz and Ehrlich (1976)
Saudi Arabia	Central part of the platform	Dhruma, Tuwaiq and Hanifa Formations	Shallow marine (lagoonal or back-reef)	Bad-preserved, dominance of *W. britannica* or *C. margerelii*; 16 species	Middle Callovian-Early Oxfordian	5°S	Manivit (1987)
Falkland Plateau	DSDP 330	Sapropelic claystone and limestone	Restricted basin	Moderate to well-preserved, dominance of *Watznaueria* or *C. margerelii*; 20 species	Oxfordian	60°S	Wise and Wind (1976)

[a] Paleolatitudes from Smith et al. (1994).

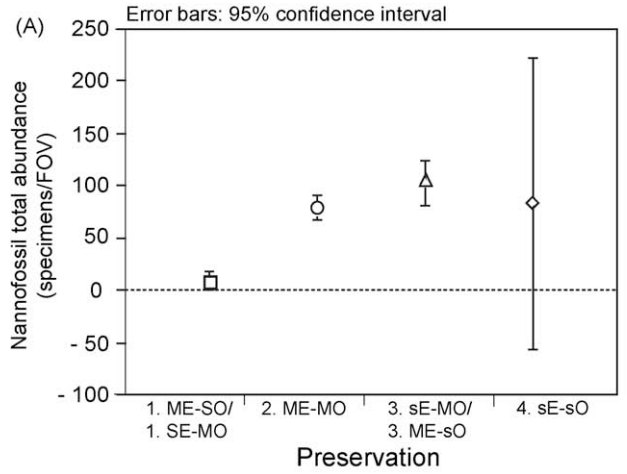

Bonferroni/Dunn Test
Significance level: 5%

	Mean diff.	Crit. diff.	Probability	
1. ME-SO/1. SE-MO *vs* 2. ME-MO	-69.709	43.053	<.0001	S
1. ME-SO/1. SE-MO *vs* 3. ME-sO/3. sE-MO	-94.216	43.053	<.0001	S
1. ME-SO/1. SE-MO *vs* 4. sE-sO	-74.461	87.440	.0236	
2. ME-MO *vs* 3. ME-sO/3. sE-MO	-24.507	30.443	.0320	
2. ME-MO *vs* 4. sE-sO	-4.752	81.970	.8749	
3. ME-sO/3. sE-MO *vs* 4. sE-sO	19.755	81.970	.5135	

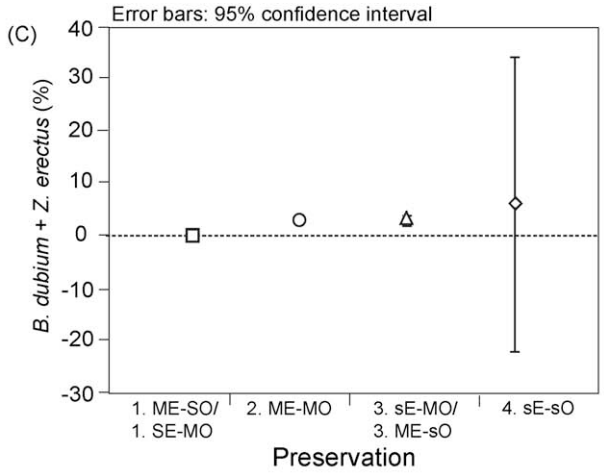

Bonferroni/Dunn Test
Significance level: 5%

	Mean diff.	Crit. diff.	Probability	
1. ME-SO/1. SE-MO *vs* 2. ME-MO	-2.566	1.960	.0007	S
1. ME-SO/1. SE-MO *vs* 3. ME-sO/3. sE-MO	-2.419	1.960	.0013	S
1. ME-SO/1. SE-MO *vs* 4. sE-sO	-5.482	3.980	.0004	S
2. ME-MO *vs* 3. ME-sO/3. sE-MO	.147	1.386	.7732	
2. ME-MO *vs* 4. sE-sO	-2.916	3.731	.0371	
3. ME-sO/3. sE-MO *vs* 4. sE-sO	-3.063	3.731	.0288	

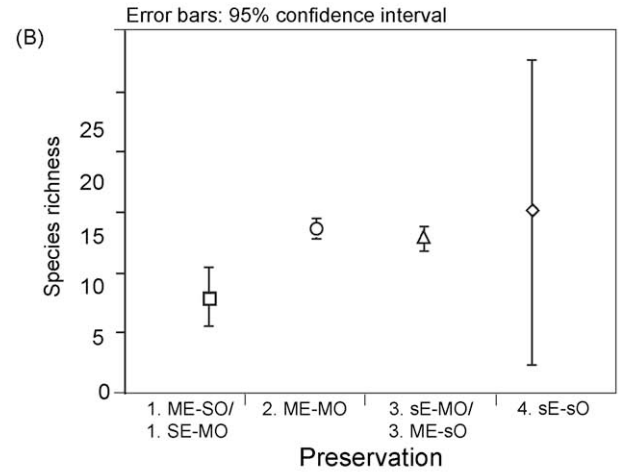

Bonferroni/Dunn Test
Significance level: 5%

	Mean diff.	Crit. diff.	Probability	
1. ME-SO/1. SE-MO *vs* 2. ME-MO	-5.630	2.563	<.0001	S
1. ME-SO/1. SE-MO *vs* 3. ME-sO/3. sE-MO	-4.852	2.563	<.0001	S
1. ME-SO/1. SE-MO *vs* 4. sE-sO	-7.000	5.205	.0005	S
2. ME-MO *vs* 3. ME-sO/3. sE-MO	.778	1.812	.2464	
2. ME-MO *vs* 4. sE-sO	-1.370	4.880	.4467	
3. ME-sO/3. sE-MO *vs* 4. sE-sO	-2.148	4.880	.2346	

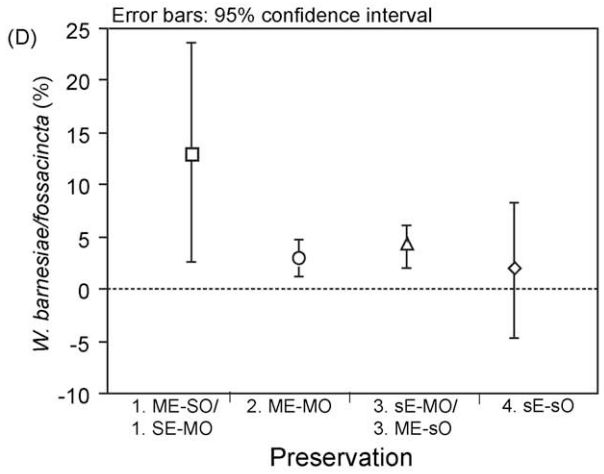

Bonferroni/Dunn Test
Significance level: 5%

	Mean diff.	Crit. diff.	Probability	
1. ME-SO/1. SE-MO *vs* 2. ME-MO	10.112	6.998	.0002	S
1. ME-SO/1. SE-MO *vs* 3. ME-sO/3. sE-MO	8.975	6.998	.0009	S
1. ME-SO/1. SE-MO *vs* 4. sE-sO	11.236	14.214	.0351	
2. ME-MO *vs* 3. ME-sO/3. sE-MO	-1.137	4.949	.5332	
2. ME-MO *vs* 4. sE-sO	1.124	13.325	.8189	
3. ME-sO/3. sE-MO *vs* 4. sE-sO	2.261	13.325	.6452	

Fig. 6. Mean nannofossil total abundance (specimens per field of view) (**A**), mean species richness (**B**), mean relative abundance of delicate taxa (*B. dubium* + *Z. erectus*) (**C**), and mean relative abundance of *W. barnesiae* (**D**) for different classes of preservation for the Chénier Ravine section. The different classes of preservation for nannofossil assemblages are: 1, SE and/or SO; 2, ME-MO; 3, sE-MO or ME-sO; 4, sE-sO; with SE: strongly etched; SO: strongly overgrown; ME: moderately etched; MO: moderately overgrown; sE: slightly etched; sO: slightly overgrown. In order to estimate the significance of the differences observed between the different classes of preservation, a Bonferroni/Dunn test is applied. It allows comparison of the means calculated for datasets with different sizes (here, the highly variable number of samples showing a different preservation state). Statistically significant differences achieved when $p < 0.0083$ for an overall experimentwise significance level $\alpha = 0.05$. Sixty-nine samples are considered in this analysis.

are observed in samples having a high degree of etching and/or overgrowth (Fig. 6(D)). For all tested parameters, differences between heavily etched and/or overgrown nannofossil assemblages and the other classes of preservation are always statistically significant; on the other hand, within the other classes of preservation, differences are observed but are not statistically significant (Fig. 6).

Samples with a high degree of etching and overgrowth are mainly located at the base of the section. Samples 1, 3, 4 and 7, corresponding to limestones, present strongly overgrown nannofossil assemblages. Preservation of nannofossils is generally poorer in limestones than in marls due to increasing diagenesis in limestone (Roth and Thierstein, 1972). Samples 11, 14 and 18, corresponding to argillaceous marls, show strong dissolution effects. Samples 1, 3, 4, 7, 11, 14 and 18 are characterized by very low nannofossil total abundance and very low species richness with respect to other samples. The delicate taxa are generally absent in these samples. The percentages of both *W. barnesiae/fossacincta* and *S. punctulata* are higher in this part than in the rest of the section. At the base of the section, a strong diagenetic alteration affects the nannofossil composition in poorly-preserved samples. Calcareous nannofossils from other samples are better preserved and more diverse. In addition, significant relative abundances of dissolution-susceptible taxa such as *B. dubium* and *Z. erectus* indicate that nannofossil fluctuations are moderately affected by diagenesis in the rest of the section.

5.2. Calcareous nannofossils and carbonate production

In the Chénier Ravine section, a negative correlation between nannofossil total abundance (specimens/field of view) and carbonate content is observed (Figs. 5 and 7).

The contribution to the pelagic carbonate content by microorganisms other than calcareous nannofossils was investigated in thin sections in various samples selected from different parts of the section (Bof, 2000; Fig. 2 and Table S2 in Appendix A). This analysis reveals that the microfauna (rare foraminifera and radiolarian, sponge spicules) had a minor contribution to the carbonate fraction both in limestones and in marls. This suggests that the carbonate fraction is not predominantly produced by microorganisms and that the pelagic carbonate production is reduced in the Chénier Ravine section. Thus, two hypotheses can be proposed: the carbonate fraction had a predominantly:

- allochthonous, carbonate-platform origin;
- or benthic and/or nektobenthic origin (Pittet et al., 2000; Pittet and Mattioli, 2002; Giraud et al., 2003; Reboulet et al., 2003, 2005; Mattioli, 2006).

The analysis of thin sections reveals that at the base of the Chénier Ravine section (Middle Callovian to the Callovian-Oxfordian transition), limestones are characterized by a small proportion of bioclasts, mainly represented by planktonic crinoids (*Saccocoma*), suggesting that the bioclastic fraction is autochthonous and not transported from the platform (Bof, 2000). In the marls, the macrofauna is characterized by fragments of benthic (crinoids, urchins, bivalves, brachiopods), nektobenthic (nautiloids: rhyncholits) and nektonic organisms (ammonites and belemnites). In the upper part of the 'Terres Noires' Formation (*cordatum* ammonite Zone; Fig. 2), the collected limestones reveal an important bioclastic fraction associated with detrital minerals. In marls, the macrofauna is composed of variable organism fragments (crinoids, bivalves, rhyncholits, Aptychi, belemnites), and the microfauna is composed of abundant sponge spicules. In this interval, a greater contribution of allochthonous carbonate can be invoked (Bof, 2000). The Chénier Ravine section is located at the transition between the slope and the basin and could have been sensitive to changes in the intensity of the carbonate import from shallower water environments. At this time, platforms lying on the submerged French Central Massif were the principal source of allochtonous carbonate sediments transported towards deeper environments (Elmi, 1967, 1990).

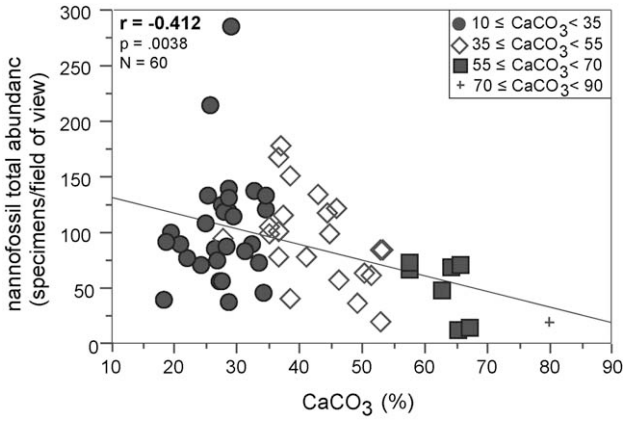

Fig. 7. Bivariate plot showing the relationship between different calcium carbonate content classes and calcareous nannofossil total abundance. Poorly preserved samples (with strongly etched and/or overgrown nannofossil assemblages) are excluded from this analysis.

These results are in agreement with those obtained by Louis-Schmid et al. (2007a). They have estimated that for the latest Early Oxfordian (*cordatum* zone) and for the Middle Oxfordian of two other basinal sections of the French Subalpine Basin (Trescléoux and Oze sections), around 20% of the carbonate is of pelagic origin. The pelagic carbonate fraction both in limestones and marls of the French Subalpine Basin is always of minor importance across the Middle-Late Jurassic transition. The non-pelagic carbonate fraction is predominantly of nektonic/benthic origin at the Callovian-Oxfordian transition and of allochthonous origin from carbonate platforms at the end of the Early Oxfordian. The carbonate platforms worldwide were affected by a major crisis in carbonate productivity at the Callovian-Oxfordian transition (Cecca et al., 2005). Two hypotheses can explain the allochthonous origin of carbonate mud in the French Subalpine Basin at the Early-Middle Oxfordian transition. First, reduced and isolated carbonate areas subsisted on the basin margins during the Early Oxfordian. Second, a partial recovery of carbonate productivity on shelves began at the end of the Early Oxfordian, linked to

better paleoenvironmental conditions (warmer surface waters and/or drier climatic conditions and reduced runoff).

5.3. Calcareous nannofossils and their paleoecological significance

The paleoecological significance of selected calcareous nannofossil taxa are summarized in Table 2.

In the Chénier Ravine section, the small-sized specimens of *W. britannica* (Morphotypes A + B) are characteristic of nannofossil assemblages of low species richness, diversity and evenness, indicative of very unstable environmental conditions where nutrients are used by a small number of dominant taxa (Watkins, 1989). The large specimens of *W. britannica* are characteristic of nannofossil assemblages of moderate species richness and diversity. Their percentages display low positive correlations with those of *C. margerelii* and *Z. erectus*. These data suggest that the large specimens of *W. britannica* are indicative of more stable environmental conditions with respect to small morphotypes, but rather in mesotrophic than oligotrophic surface waters.

For the Jurassic period, Lees et al. (2006) have observed in pristinely preserved samples in the Kimmeridge Clay Formation that abundance peaks of *Z. erectus* and *Biscutum* spp. only occur during the switchovers between the dominant watznaueriaceans. Walsworth-Bell (2001) has observed in the Oxford Clay Formation (Middle Callovian-Early Oxfordian) an increase in the relative abundance of *Biscutum* spp. and *Z. erectus* associated with an increase in the species diversity and a decrease in the relative abundance of *W. britannica*. In the Chénier Ravine section, *B. dubium* is characteristic of nannofossil assemblages of moderate species richness, Shannon diversity and evenness, and *Z. erectus* is less abundant than the other small placoliths described before. In the Callovo-Oxfordian marine paleoenvironments of the French Subalpine Basin, when trophic levels in surface waters became very high, *Z. erectus* and *B. dubium* probably did not compete for nutrients with respect to *W. britannica*. Highest relative abundances of *B. dubium* and *Z. erectus* observed just above the Callovian-Oxfordian boundary can be explained both by increased nutrient input and cooler surface waters as they are generally associated with nutrient-richer but also cooler surface waters (Table 2).

The paleoecological affinities of *W. manivitiae/britannica* are still unclear, as its relative abundance does not present any significant correlations with other variables. However, higher relative abundances are recorded at the end of the Early Oxfordian, characterized by low nannofossil total abundances (specimens per field of view), species richness and diversity, associated with the highest relative abundance of small-sized *W. britannica*. This suggests that *W. manivitiae/britannica* could live in unstable conditions.

5.4. Variation with time of calcareous nannofossil assemblages and relationships with paleoenvironmental parameters

From the Middle Callovian (*coronatum* ammonite Zone) through to the Callovian-Oxfordian boundary, the calcium carbonate content drastically decreases (Fig. 2). Nannofossil assemblages are sometimes strongly altered by diagenetic overprint both in limestones and marls. Low calcareous nannofossil total abundances are recorded (Fig. 2). The assemblages show a great contribution of small morphotypes of *W. britannica* (Fig. 4). *Cyclagelosphaera margerelii* relative abundance increases in this interval, which can be explained by a sea level minimum recorded within the *lamberti* ammonite Zone (Dromart et al., 2003). The low proportion of bioclasts,

Table 2
Paleoecological significance of selected nannofossil taxa. Data from: **1**, Pittet and Mattioli (2002); **2**, Walsworth-Bell (2001); **3**, Lees et al. (2006); **4**, Olivier et al. (2004); **5**, Tremolada et al. (2006); **6**, Giraud et al. (2006); **7**, Bown (2005); **8**, Giraud et al. (2005); **9**, Premoli Silva et al. (1989); **10**, Erba (1991); **11**, Coccioni et al. (1992); **12**, Herrle (2003); **13**, Giraud et al. (2003); **14**, Roth (1981); **15**, Roth and Bowdler (1981); **16**, Roth and Krumbach (1986); **17**, Mutterlose and Kessels (2000); **18**, Bartolini et al. (2003).

Nannoplankton paleoecological indices	Nutrient concentration	Ecological strategy	Paleoceanography
Watznaueria britannica	High mesotrophic [1]	R-selected [2, 3]	
Small morphotypes	Meso-eutrophic [4, 5, 6]		Very unstable conditions [this study]
Large morphotypes	Oligotrophic [4, 5, 6]		
	Mesotrophic [this study]		
Cyclagelosphaera margerelii	Mesotrophic [1]	R-selected [3]	Preference for neritic and/or restricted conditions [7, 8]
Lotharingius hauffii	Meso-eutrophic [1, 4]		
Discorhabdus spp.	Meso-eutrophic [9, 10, 11, 12, 13]		
Biscutum spp.	Eutrophic [14, 15, 16]		Oceanic sites of upwelling/shelf areas with storm mixing [14, 15, 16]
			Cooler surface waters [16, 17]
Zeugrhabdotus erectus	Eutrophic [14, 15, 16]		Oceanic sites of upwelling/shelf areas with storm mixing [14, 15, 16]
			Cooler surface waters [16, 17]
A-group	Meso-eutrophic [4]		Cooler surface waters [4]
Watznaueria manivitiae	Oligotrophic [1]		Warm surface waters [2, 18]
Watznaueria manivitiae/britannica			Unstable conditions [this study]

the abundance of spumellar radiolarians and sponge spicules in the micropaleontological content and the strong bioturbation of beds suggest a low sedimentation rate in a relatively proximal paleoenvironment (Bof, 2000).

Across the Callovian-Oxfordian boundary, moderate total abundances are recorded (Fig. 2) and associated with a successive maximum relative abundance in the group of small coccoliths (A-group, *Biscutum* spp., *Z. erectus* and *Discorhabdus* spp., respectively; Fig. 4). This could be indicative of mesotrophic conditions and a thermal minimum in surface waters. Relatively humid climate may have enhanced both runoff from the hinterland and nutrient input in the marine realm. Terrigenous inputs originated partly from the submarine erosion of the French Central Massif Hercynian basement and its Triassic siliciclastic sediment cover (Elmi, 1967, 1990; Fig. 1). Colour banding is recognized in the Early Oxfordian 'Terres Noires' Formation and attributed to periodic monsoon-type climates (Tribovillard, 1989). At that time, more humid and cooler climatic conditions are attested in the boreal domain (Abbink et al., 2001) and in Western Europe, by the presence of *Xenoxylon* plants (Philippe and Thévenard, 1996). Higher nannofossil total abundances are recorded for that period, associated with a sharp increase of small-sized *W. britannica*, suggesting higher productivity in surface waters with respect to the Callovian-Oxfordian boundary. The decrease in Shannon diversity and in the relative abundances of small placoliths suggests that paleoenvironmental conditions became less favourable for the nannoplankton community (eutrophic conditions; Figs. 2 and 4).

The middle part of the Early Oxfordian (*mariae-cordatum* ammonite Zone transition in the Chénier Ravine) is characterized by a progressive decrease in nannofossil total abundance and diversity indices and an increase in calcium carbonate content (Fig. 2). The increasing carbonate content is not linked to calcareous nannofossils, as their productivity decreases. The decrease in siliciclastic inputs from the proximal areas can explain the increase in carbonate content in the Chénier Ravine section. Decreased runoff and associated nutrients could also lead to reduced nannoplankton productivity. The relative abundances of almost all nannofossil taxa decrease during this interval, except those of the smallest-sized specimens of *W. britannica* (Morphotype A) and of *W. manivitiae/britannica* (Fig. 4). Unfavourable paleoenvironmental conditions (always cooler but drier climatic conditions and associated nutrient-depleted surface waters) for the nannoplankton prevailed during this interval.

From the end of the Early Oxfordian until the early Middle Oxfordian, the calcium carbonate content increases (Fig. 2). Important bioclastic fraction and siliciclastic minerals found in the sediments suggest enhanced detritic input from the surrounding proximal areas (Bof, 2000). The sharp increase in the relative abundances of *Discorhabdus* spp. and of *L. hauffii* indicates that mesotrophic conditions prevailed in the surface waters (Fig. 4). The decrease in the relative abundance of the A-group from the upper part of the *cordatum* zone suggests that surface waters were certainly warmer from the end of the Early Oxfordian (Fig. 4). At the Early-Middle Oxfordian transition, more favourable conditions (warmer and mesotrophic surface waters) prevailed, allowing a partial recovery of carbonate productivity both on platforms and in the pelagic environment. The total recovery of platform carbonate production, and in particular, the large development of coral reefs, occurred at the onset of the *transversarium* ammonite Zone, when widespread eustatic rise and warming are recorded (Middle Oxfordian; e.g., Cecca et al., 2005).

6. Conclusions

The study of temporal distribution patterns of calcareous nannofossil assemblages in the French Subalpine Basin across the Middle-Late Jurassic transition has revealed the following features:

- in the Middle-Late Callovian interval, the nannofossil composition is often controlled by preservation, whereas in the rest of the section, it represents a primary signal that is slightly to moderately altered by diagenetic overprint;
- the assemblages are constantly dominated by *Watznaueria britannica*;
- an increase in surface water productivity is demonstrated by both an increase in nannofossil total abundance and in the relative abundance of taxa adapted to high-trophic levels across the Callovian-Oxfordian boundary (as already shown by Tremolada et al., 2006 in the eastern Paris Basin); it is not restricted to one basin. Further studies will be necessary to demonstrate whether this is global. This event is also coincident in the French Subalpine Basin with a cooling of surface waters as indicated by an increase in the relative abundance of cool-water taxa. Increased precipitation and runoff under contrasted seasonal climatic conditions (monsoon-type) lead to eutrophication of marine surface waters in the French Subalpine Basin. Then, decreased runoff and associated nutrient-depleted surface waters, certainly linked to drier climatic conditions, lead to a decrease in calcareous nannofossil productivity during the middle part of the Early Oxfordian (*mariae-cordatum* ammonite Zone transition). At the Early-Middle Oxfordian transition, more favourable conditions for the nannofossil community (warmer and mesotrophic surface waters) prevail;
- the nannofossil carbonate production is limited both in limestones and marls. The carbonate fraction is predominantly of nektonic/benthic origin at the Callovian-Oxfordian transition, and of allochthonous origin from carbonate platforms at the Early Oxfordian-Middle Oxfordian transition. Two hypotheses are proposed to explain the allochthonous (platform) origin for the carbonate fraction:
  - reduced isolated shallow carbonate platform areas subsisting on the margins of the French Subalpine Basin during the Early Oxfordian,
  - a partial recovery of carbonate productivity on shallow platforms begins at the Early Oxfordian-Middle Oxfordian transition in south-eastern France.

Acknowledgements

We thank Paula Desvignes (Lyon) for smear slide preparation and calcimetric analyses. We are extremely grateful to Stéphane Guillot, Emanuela Mattioli and Bernard Pittet for stimulating discussions. The manuscript was considerably improved following the comments of two anonymous reviewers. This work is a contribution to the team project 'Quantification of productivities and transfers in the Mesozoic' of the CNRS-UMR 5125 'Paléoenvironnements et Paléobiosphère', Lyon.

Appendix A. Supplementary data

Supplementary data (Tables S1 and S2) associated with this article can be found, in the online version, at doi:10.1016/j.geobios.2009.05.002.

Appendix B. List of species cited in the text, figures and dataset (Appendix A):

Axopodorhabdus cylindratus (Noël, 1965) Wind and Wise in Wise and Wind, 1977 (Fig. 3(1))
Biscutum dubium (Noël, 1965) Grün in Grün et al., 1974 (Fig. 3(2))
Crepidolithus crassus (Deflandre, 1954) Noël, 1965
C. perforata (Medd, 1979) Grün and Zweili, 1980
Cyclagelosphaera margerelii (Noël, 1965) (Fig. 3(3))
C. wiedmannii Reale and Monechi, 1994
Discorhabdus sp. (Fig. 3(4)).

Description: A species of *Discorhabdus* with a circular to subcircular outline, ranging from 3 to 4.5 µm. Coccoliths are composed of at least 20 radial, non-imbricate elements. The central area is open and variable in size. In crossed nicols, the inner ring is brighter than the rim as in *D. criotus*, but the presence of another birefringent central element cycle suggests the presence of a small inner spine.

D. patulus (Deflandre in Deflandre and Fert, 1954) Noël, 1965 (Fig. 3(5))
D. striatus Moshkovitz and Ehrlich, 1976 (Fig. 3(6))
Ethmorhabdus gallicus Noël, 1965 (Fig. 3(7))
Lotharingius crucicentralis (Medd, 1971) Grün and Zweili, 1980
L. hauffii Grün and Zweili in Grün et al., 1974 (Fig. 3(8))
Polypodorhabdus escaigii Noël, 1965 (Fig. 3(9))
Similiscutum novum (Goy, 1979) Mattioli et al., 2004
Stephanolithion bigotii ssp. *bigotii* Deflandre, 1939
S. bigotii Deflandre, 1939 ssp. *maximum* Medd, 1979 (Fig. 3(10))
Triscutum expansus (Medd, 1979) Dockerill, 1987
Tubirhabdus patulus Rood et al., 1973
Watznaueria barnesiae (Black, 1959) Perch-Nielsen, 1968 (Fig. 3(11))
Watznaueria aff. *barnesiae* (Fig. 3(12)).

Description: Large elliptical to subcircular coccoliths. In crossed-nicols, *W.* aff. *barnesiae* shows yellow colours. It is very similar in general structure (included the central area) to *W. barnesiae*, but the coccolith size is larger (diameter 7–9 µm) and the birefringence is higher, but lower than for *W. manivitiae*.

Remarks: The high birefringence could be due to recristallisation.

W. britannica (Stradner, 1963) Reinhardt, 1964 (Fig. 3 (13–19)).

Remarks: The different morphotypes A–F described in Giraud et al. (2006) are present in the assemblages.Another new morphotype, called G, characterized by a very large central area spanned by a small bridge with a button-shaped, is recognized.

W. communis Reinhardt, 1964
W. fossacincta (Black, 1971) Bown in Bown and Cooper, 1989
W. manivitiae Bukry, 1973 (Fig. 3(22))
W. manivitiae/britannica (Fig. 3(20)).

Description: A large (diameter > 8 µm) and highly birefringent *Watznaueria* with a large external cycle. The central area is small and spanned by a button-shaped bridge (characteristic of *W. britannica*). It is very similar in morphology to *W. manivitiae*.

Watznaueria sp. 3 (Erba, 1990)
Watznaueria sp. 4 (Erba, 1990)
Zeugrhabdotus embergeri (Noël, 1958) Perch-Nielsen, 1984
Z. erectus (Deflandre in Deflandre and Fert, 1954) Reinhardt, 1965 (Fig. 3(21))
Incertae sedis
Schizosphaerella punctulata Deflandre and Dangeard, 1938 (Fig. 3(23)).

References

Abbink, O., Targarona, J., Brinkhuis, H., Visscher, H., 2001. Late Jurassic to earliest Cretaceous palaeoclimatic evolution of the southern North Sea. Global and Planetary Change 30, 231–256.

Artru, P., 1972. Les Terres Noires du bassin rhodanien (Bajocien supérieur à Oxfordien moyen). Stratigraphie – Sédimentologie – Géochimie. PhD Thesis, Université Claude-Bernard Lyon-1 (unpublished).

Baccelle, L., Bosellini, A., 1965. Diagrammi per la stima visiva della composizione percentuale nelle rocce sedimentarie. Annali dell'Università di Ferrara, Sezione IX Scienze Geologiche e Paleontologiche 1, 59–62.

Bartolini, A., Pittet, B., Mattioli, E., Hunziker, J.C., 2003. Regional control on stable isotope signature in deep-shelf sediments: an example of the Late Jurassic of southern Germany (Oxfordian-Kimmeridgian). Sedimentary Geology 160, 107–130.

Bof, E., 2000. Rhyncholites (parties antérieures calcifiées de la mâchoire supérieure des Nautilida) callovo-oxfordiens du Chénier ; interprétation paléoécologique. Mémoire Maîtrise, université Claude-Bernard Lyon-1 (unpublished).

Bornemann, A., Mutterlose, J., 2006. Size analyses of the coccolith species *Biscutum constans* and *Watznaueria barnesiae* from the Late Albian

''Niveau Breistroffer'' (SE France): taxonomic and palaeoecological implications. Geobios 39, 599–615.

Bouhamdi, A., Gaillard, C., Ruget, C., Bonnet, L., 2000. Foraminifères benthiques de l'Oxfordien moyen de la plate-forme au bassin dans le Sud-Est de la France, Répartition et contrôle environnemental. Eclogae Geologicae Helvetiae 93, 315–330.

Bown, P.R., 2005. Selective calcareous nannoplankton survivorship at the Cretaceous-Tertiary boundary. Geology 33, 653–656.

Bown, P.R., Cooper, M.K.E., Lord, A.R., 1988. A calcareous nannofossil biozonation scheme for the early to mid Mesozoic. Newsletter Stratigraphy 20, 91–114.

Bown, P.R., Cooper, M.K.E., 1998. Jurassic. In: Bown, P.R. (Ed.), Calcareous Nannofossil Biostratigraphy. British Micropalaeontological Society Series, Kluwer Academic Press, Dordrecht, pp. 34–85.

Bown, P.R., Young, J.R., 1997. Mesozoic calcareous nannoplankton classification. Journal of Nannoplankton Research 19, 21–36.

Cecca, F., Martin Garin, B., Marchand, D., Lathuilière, B., Bartolini, A., 2005. Paleoclimatic control of biogeographic and sedimentary events in Tethyan and peri-Tethyan areas during the Oxfordian (Late Jurassic). Palaeogeography, Palaeoclimatology, Palaeoecology 222, 10–32.

Charbonnier, S., Vannier, J., Gaillard, C., Bourseau, J.-P., Hantzpergue, P., 2007. The La Voulte Lagerstätte (Callovian): Evidence for a deep water setting from sponge and crinoid communities. Palaeogeography, Palaeoclimatology, Palaeoecology 250, 216–236.

Coccioni, R., Erba, E., Premoli Silva, I., 1992. Barremian-Aptian calcareous plankton biostratigraphy from the Gorgo Cerbara section (Marche, central Italy) and implications for plankton evolution. Cretaceous Research 13, 517–537.

Dardeau, G., Atrops, F., Fortwengler, D., de Graciansky, P.C., Marchand, D., 1988. Jeu de blocs et tectonique distensive au Callovien et à l'Oxfordien dans le bassin du Sud-Est de la France. Bulletin de la Société géologique de France 4, 771–777.

Dardeau, G., Marchand, D., Fortwengler, D., 1994. Tectonique synsédimentaire et variations du niveau marin pendant le dépôt de la formation des Terres Noires (Callovien supérieur-Oxfordien moyen ; bassin du Sud-Est, France). Comptes Rendus de l'Académie des Sciences de Paris 319, 559–565.

Debrand-Passard, S., Courbouleix, S., Lienhardt, M.J., 1984. Synthèse géologique du Sud-Est de la France. Bureau de Recherches Géologiques et Minières. Mémoire 125, 1–615.

Dromart, G., Garcia, J.-P., Picard, S., Atrops, F., Lécuyer, C., Sheppard, S.M.F., 2003. Ice age at the Middle-Late Jurassic transition? Earth and Planetary Science Letters 213, 205–220.

Elmi, S., 1967. Le Lias supérieur et le Jurassique moyen de l'Ardèche. Documents des Laboratoires de Géologie de Lyon 19, 1–507.

Elmi, S., 1990. Stages in the evolution of late Triassic and Jurassic carbonate platforms: the western margin of the Subalpine Basin (Ardèche, France). In: Tucker, M.E., Wilson, J.L., Crevello, P.D., Sarg, J.R., Read, J.F. (Eds.), Carbonate platforms, facies, sequences and evolution. Blackwell Scientific publications, Oxford, pp. 109–144.

Erba, E., 1991. Calcareous nannofossil distribution in pelagic rhythmic sediments (Aptian-Albian Piobbico core, Central Italy). Rivista Italiana di Paleontologia e Stratigrafia 97, 455–484.

Frontier, S., Pichod-Viale, D., 1998. Ecosystèmes, structures fonctionnement évolution. Dunod Press, Paris.

Giraud, F., Courtinat, B., Atrops, F., 2009. Spatial distribution patterns of calcareous nannofossils across the Callovian-Oxfordian transition in the French Subalpine Basin. Marine Micropaleontology 72, 129–145.

Giraud, F., Courtinat, B., Garcia, J.-P., Baudin, F., Guillocheau, F., Dromart, G., Atrops, F., Colleté, C., 2005. Palynofacies and calcareous nannofossils in the Upper Kimmeridgian, southeastern Paris Basin (France). Bulletin de la Société géologique de France 176, 457–466.

Giraud, F., Olivero, D., Baudin, F., Reboulet, S., Pittet, B., Proux, O., 2003. Minor changes in surface water fertility across the Oceanic Anoxic Event 1d (latest Albian, SE France) evidenced by calcareous nannofossils. International Journal of Earth Sciences 92, 267–284.

Giraud, F., Pittet, B., Mattioli, E., Audouin, V., 2006. Paleoenvironmental controls on morphology and abundance of the coccolith *Watznaueria britannica* (Late Jurassic, southern Germany). Marine Micropaleontology 60, 205–225.

de Graciansky, P.C., Dardeau, G., Bodeur, Y., Elmi, S., Fortwengler, D., Jacquin, T., Marchand, D., Thierry, J., 1999. Les Terres Noires du Sud-Est de la France (Jurassique moyen et supérieur) : interprétation en termes de stratigraphie séquentielle. Bulletin du Centre de Recherches d'Exploration-Production Elf-Aquitaine 22, 35–69.

Hamilton, G.B., 1978. Calcareous nannofossils from the Upper Callovian and Lower Oxfordian (Jurassic) of Staffin Bay, Isle of Skye, Scotland. Proceedings of the Yorkshire Geological Society 42, 29–39.

Herngreen, G.F.W., De Boer, K.F., Romein, B.J., Lissenberg, T.H., Wijker, N.C., 2000. Middle Callovian beds in the Achterhoek, eastern Netherlands. Mededelingen Rijks Geologische Dienst 37, 95–123.

Herrle, J.O., 2003. Reconstructing nutricline dynamics of mid-Cretaceous oceans: evidence from calcareous nannofossils from the Niveau Paquier black shale (SE France). Marine Micropaleontology 47, 307–321.

Hill, M.E., 1975. Selective dissolution of mid-Cretaceous (Cenomanian) calcareous nannofossils. Micropaleontology 21, 227–235.

Hotinski, R.M., Toggweiler, J.R., 2003. Impact of a Tethyan circumglobal passage on ocean heat transport and ''equable'' climates. Paleoceanography 18, 1007, doi:10.1029/2001PA000730.

Jones, C.E., Jenkyns, H.C., Coe, A.L., Hesselbo, S.P., 1994. Strontium isotopes in Jurassic and Cretaceous seawater. Geochimica Cosmochimica Acta 58, 3061–3074.

de Kaenel, E., Bergen, J.-A., von Salis Perch-Nielsen, K., 1996. Jurassic calcareous nannofossil biostratigraphy of western Europe: compilation of recent studies and calibration of bioevents. Bulletin de la Société géologique de France 167, 3–14.

Lees, J.A., Bown, P.R., Mattioli, E., 2005. Problems with proxies? Cautionary tales of calcareous paleoenvironmental indicators. Micropaleontology 51, 333–343.

Lees, J.A., Bown, P.R., Young, J.R., 2006. Photic zone palaeoenvironments of the Kimmeridge Clay Formation (Upper Jurassic, UK) suggested by calcareous nannoplankton palaeoecology. Palaeogeography, Palaeoclimatology, Palaeoecology 235, 110–134.

Lees, J.A., Bown, P.R., Young, J.R., Riding, J.B., 2004. Evidence for annual records of phytoplankton productivity in the Kimmeridge Clay Formation coccolith stone bands (Upper Jurassic, Dorset, UK). Marine Micropaleontology 52, 29–49.

Lemoine, M., de Graciansky, P.C., 1988. Marge continentale téthysienne dans les Alpes. Bulletin de la Société géologique de France 4, 597–797.

Louis-Schmid, B., Rais, P., Schaeffer, P., Bernasconi, S.M., Pellenard, P., Collin, P.-Y., Weissert, H., 2007a. Detailed record of the mid-Oxfordian (Late Jurassic) positive carbon-isotope excursion in two hemipelagic sections (France and Switzerland): A plate tectonic trigger? Palaeogeography, Palaeoclimatology, Palaeoecology 248, 459–472.

Louis-Schmid, B., Rais, P., Schaeffer, P., Bernasconi, S.M., Weissert, H., 2007b. Plate tectonic trigger of changes in pCO_2 and climate in the Oxfordian (Late Jurassic): Carbon isotope and modelling evidence. Earth and Planetary Science Letters 258, 44–60.

Manivit, H., 1987. Distribution de nannofossiles calcaires du Jurassique moyen et supérieur en Arabie Saoudite centrale. In: Enay, R. (Ed.), Le Jurassique d'Arabie Saoudite Centrale, 9. Geobios MS, pp. 277–291.

Mattioli, E., 1997. Nannoplankton productivity and diagenesis in the rhythmically bedded Toarcian-Aalenian Fiuminata section (Umbria-Marche Apennine, central Italy). Palaeogeography, Palaeoclimatology, Palaeoecology 130, 113–133.

Mattioli, E., 2006. Le nannoplancton calcaire durant l'événement anoxique du Toarcien inférieur : implications pour la paléocéanographie de la Téthys occidentale. Mémoire d'habilitation à diriger des recherches, université Claude-Bernard Lyon-1 (unpublished).

Medd, A.W., 1979. The Upper Jurassic coccoliths from Haddenham and Gamlingay boreholes (Cambridgeshire, England). Eclogae Geologicae Helvetiae 72, 19–109.

Moshkovitz, S., Ehrlich, A., 1976. Distribution of middle and upper Jurassic calcareous nannofossils in the northeastern Negev, Israel and in Gerel Maghara, northern Sinai. Geological Survey Israel Bulletin 69, 1–47.

Mutterlose, J., Kessels, K., 2000. Early Cretaceous calcareous nannofossils from high latitudes: implications for palaeobiogeography and palaeoclimate. Palaeogeography, Palaeoclimatology, Palaeoecology 160, 347–372.

Nyman, T., Razin, P., Bonijoly, D., Le Strat, P., Courel, L., Poli, E., Dromart, G., Elmi, S., 1996. Stratigraphic record of the structural evolution of the western extensional margin of the Subalpine Basin during the Triassic and Jurassic, Ardèche, France. Marine Petroleum Geology 13, 625–652.

Olivier, N., Pittet, B., Mattioli, E., 2004. Palaeoenvironmental control on sponge-microbialite reefs and contemporaneous deep-shelf marl-limestone deposition (Late Oxfordian, southern Germany). Palaeogeography, Palaeoclimatology, Palaeoecology 212, 233–263.

Perch-Nielsen, K., 1985. Mesozoic calcareous nannofossils. In: Bolli, H.M., Saunders, J.B., Perch-Nielsen, K. (Eds.), Plankton Stratigraphy. Cambridge University Press, Cambridge, pp. 329–426.

Philippe, M., Thévenard, F., 1996. Distribution and palaeoecology of the Mesozoic wood genus *Xenoxylon*: palaeoclimatological implication for the Jurassic of Europe. Review of Palaeobotany and Palynology 91, 353–370.

Pittet, B., Strasser, A., Mattioli, E., 2000. Depositional sequences in deep-shelf environments: a response to sea-level changes and shallow-platform carbonate productivity (Oxfordian, Germany and Spain). Journal of Sedimentary Research 70, 392–407.

Premoli Silva, I., Erba, E., Tornaghi, M.E., 1989. Paleoenvironmental signals and changes in surface fertility in Mid Cretaceous Corg-rich pelagic facies of the Fucoid Marls (Central Italy). In: Cotillon, P. (Ed.), Les évènements de la partie moyenne du Crétacé (Aptien à Turonien), 11. Geobios, MS, pp. 225–236.

Pittet, B., Mattioli, E., 2002. The carbonate signal and calcareous nannofossil distribution (Balingen-Tieringen section, Late Oxfordian, south Germany). Palaeogeography, Palaeoclimatology, Palaeoecology 179, 73–98.

Rahman, A., Roth, P.H., 1992. New calcareous nannofossil taxa of Jurassic and early Cretaceous age from the Oka River region in Central Russia. Neues Jahrbuch für Geologie und Paläontologie Abhandlungen 184, 251–277.

Reboulet, S., Giraud, F., Proux, O., 2005. Ammonoid abundance variations related to changes in trophic conditions across the Oceanic Anoxic Event 1d (Latest Albian, SE France). Palaios 20, 121–141.

Reboulet, S., Mattioli, E., Pittet, B., Baudin, F., Olivero, D., Proux, O., 2003. Ammonoid and nannoplankton abundance in Valanginian (early Cretaceous) limestone-marl successions from the southeast of France basin: carbonate dilution or productivity? Palaeogeography, Palaeoclimatology, Palaeoecology 201, 113–139.

Roth, P.H., 1981. Mid-Cretaceous calcareous nannoplankton from the Central Pacific: Implications for paleoceanography. In: Thiede, J., et al. (Eds.), Initial Reports of the Deep Sea Drilling Project 62. U.S. Government Printing Office, Washington, pp. 471–489.

Roth, P.H., 1983. Jurassic and Lower Cretaceous calcareous nannofossils in the western North Atlantic (Site 534): biostratigraphy, preservation, and some observations on biogeography and paleoceanography. In: Sheridan, R.E., Gradstein, F.M., et al. (Eds.), Initial Reports of the Deep Sea Drilling Project 76. U.S. Government Printing Office, Washington, pp. 587–621.

Roth, P.H., Bowdler, J., 1981. Middle Cretaceous nannoplankton biogeography and oceanography of the Atlantic Ocean. In: Warme, J.E., Douglas, R.G., Winterer, E.L. (Eds.), The Deep Sea Drilling Project: a Decade of Progress. SEPM Society for Sedimentary Geology, Special Publications 32, Tulsa, pp. 517–546.

Roth, P.H., Krumbach, K.R., 1986. Middle Cretaceous calcareous nannofossil biogeography and preservation in the Atlantic and Indian oceans: implications for paleoceanography. Marine Micropaleontology 10, 235–266.

Roth, P.H., Thierstein, H.R., 1972. Calcareous nannoplankton: Leg 14 of the Deep Sea Drilling Project. In: Hayes, D.E., Pimm, A.C., et, al. (Eds.), Initial Reports of the Deep Sea Drilling Project 14. U.S. Government Printing Office, Washington, pp. 421–486.

Shannon, C.E., Weaver, W., 1949. The mathematical Theory of Communication. University of Illinois Press, Urbana.

Smith, A.G., Smith, D.G., Funnell, B.M., 1994. Atlas of Mesozoic and Cenozoic Coastlines. Cambridge University Press, Cambridge.

Stampfli, G.M., Borel, G.D., Cavazza, W., Mosar, J., Ziegler, P.A., 2001. The Paleotectonic Atlas of the Peri-Tethyan Domain (CD-ROM): European Geophysical Society http://www.copernicus.org/EGS/egs_info/book.htm [consulted 27.07.07].

Stille, P., Steinmann, M., Riggs, S.R., 1996. Nd isotope evidence for the evolution of the paleocurrents in the Atlantic and Tethys Oceans during the past 180 Ma. Earth and Planetary Science Letters 144, 9–19.

Thierstein, H.R., 1980. Selective dissolution of Late Cretaceous and Earliest Tertiary calcareous nannofossils: experimental evidence. Cretaceous Research 2, 165–176.

Thierstein, H.R., 1981. Late Cretaceous nannoplankton and the change at the Cretaceous-Tertiary boundary. SEPM Society for Sedimentary Geology, Special Publications 32, 355–394.

Tremolada, F., Erba, E., van de Schootbrugge, B., Mattioli, E., 2006. Calcareous nannofossil changes during the late Callovian-early Oxfordian cooling phase. Marine Micropaleontology 59, 197–209.

Tribovillard, N.-P., 1989. Contrôles de la sédimentation marneuse en milieu pélagique semi-anoxique. Exemples dans le Mésozoïque du Sud-Est de la France et de l'Atlantique. Documents des Laboratoires de Géologie de Lyon 109, 1–119.

Walsworth-Bell, E.B., 2001. Jurassic calcareous nannofossils and environmental cycles. PhD Thesis, University College London, London (unpublished).

Watkins, D.K., 1989. Nannoplankton productivity fluctuations and rhythmically-bedded pelagic carbonates of the Greenhorn Limestone (Upper Cretaceous). Palaeogeography, Palaeoclimatology, Palaeoecology 74, 75–86.

Williams, J.R., Bralower, T.J., 1995. Nannofossil assemblages, fine fraction isotopes, and the paleoceanography of the Valanginian-Barremian (Early Cretaceous) North Sea Basin. Paleoceanography 10, 815–839.

Wise Jr., S.W., Wind, F.H., 1976. Mesozoic and Cenozoic calcareous nannofossils recovered by DSDP Leg 36 Drilling on the Falkland Plateau, Southwest Atlantic Sector of the Southern Ocean. In: Barker, P.F., Dalziel, I.W.D. (Eds.), Initial Reports of the Deep Sea Drilling Project 36. U.S. Government Printing Office, Washington, pp. 269–492.